ACS OMEGA

Article

http://pubs.acs.org/journal/acsodf

Construction of Polymer-Stabilized Automatic MultiDomain Vertical Molecular Alignment Layers with Pretilt Angles by Photopolymerizing Dendritic Monomers under Electric Fields

Won-Jin Yoon,[†] Yu-Jin Choi,[†] Dong-Gue Kang,[†] Dae-Yoon Kim,[†] Minwook Park,[†] Ji-Hoon Lee,[‡] Shin-Woong Kang,[§] Seung Hee Lee,[§] and Kwang-Un Jeong*[,†]

[†]BK21 Plus Haptic Polymer Composite Research Team & Department of Polymer-NanoScience and Technology, [‡]Division of Electronics Engineering and [§]Department of BIN Convergence Technology, Chonbuk National University, Jeonju 54896, Korea

Supporting Information

ABSTRACT: The synthesized itaconic acid-based dendritic amphiphile ($Ita3C_{12}$) monomers and the methacryl polyhedral oligomeric silsesquioxane (MAPOSS) cross-linkers were directly introduced for the construction of automatic vertical alignment (auto-VA) layers in the host nematic liquid crystal (NLC) medium. The auto-VA layer can be stabilized by irradiating UV light. For the automatic fabrication of a polymer-stabilized multidomain VA (PS auto-MDVA) layer with a pretilt angle, $Ita3C_{12}$ and MAPOSS were photopolymerized under the electric field by irradiating UV light on the multidomain electrode cell. Mainly because of the pretilted NLC at zero voltage, the electro-optic properties of the PS auto-MDVA cell were dramatically improved. From the morphological observations combined with surface chemical analyses, it was found that various sizes of protrusions on the solid substrates were automatically constructed by the two-step mechanisms. We demonstrated the PS auto-MDVA cell with the enhancement of electro-optic properties as a single-step process and investigated how the protrusions were automatically developed during the polymer stabilization.

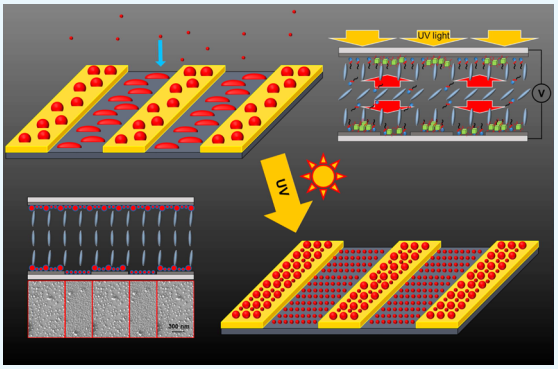

INTRODUCTION

Liquid crystals (LCs) have been widely studied and used in numerous applications, especially in display industry, because of several advantages, such as low power consumption, lightweight, thinness, and low manufacturing cost.[1−5] The LC display (LCD) is classified by types of LC alignment and electrode technique.[6−8] Various advanced LCD technologies have been developed for twisted nematic,[9,10] vertical alignment (VA),[11,12] in-plane switching,[13] and fringe-field switching[14,15] modes. Among them, the VA mode of LCD shows not only advantages in the high contrast ratio and simple process but also some technical drawbacks, such as slow response time and narrow viewing angle.[16−20] Therefore, the polymer-stabilized VA (PSVA) mode was suggested to overcome these limitations and to improve the electro-optic properties, such as fast response time, low power consumption, and wide viewing angle. The conventional PSVA mode needs additional processes even after the formation of VA layer: doping a small amount of reactive monomers in the host nematic liquid crystal (NLC) medium and subsequently polymer-stabilizing under an electric field larger than the threshold voltage for memorizing the pretilt angle of the host LC molecules. The fine modification of the pretilt angle is of importance for reducing the response times in the PSVA mode.[21−26]

In our previous work, itaconic acid-based dendritic amphiphile ($Ita3C_{12}$) monomers were newly designed and synthesized for the construction of automatic VA (auto-VA) layers in the LC cell.[1] It was found that the auto-VA layers were successfully fabricated by directly introducing $Ita3C_{12}$ in the NLC medium. $Ita3C_{12}$, which was initially dissolved in the host NLC medium, was gradually migrated toward the substrate for the formation of self-assembled monolayers, which induced the VA of host NLC medium from surface to bulk. The constructed auto-VA layer exhibited a strong surface anchoring energy (1.404×10^{-4} J/m^2) after polymer stabilization with a methacryl polyhedral oligomeric silsesquioxane (MAPOSS) cross-linker. Furthermore, the auto-VA layer after polymer stabilization was thermally stable even though the temperature of the host NLC medium was increased to nematic−isotropic transition temperature (T_{NI}). However, the polymer-stabilized automatic vertical alignment (PS auto-VA) cell without the pretilt angle of NLC directors cannot be applied as a real LCD device due to the slow response time, the increased threshold voltage, and the narrow viewing angle.

Received: July 28, 2017
Accepted: September 5, 2017
Published: September 19, 2017

DOI: 10.1021/acsomega.7b01015
ACS Omega 2017, 2, 5942−5948

In this study, we successfully demonstrated the automatic fabrication of polymer-stabilized multidomain VA layers with pretilted NLC medium (polymer-stabilized multidomain VA (PS auto-MDVA)) by polymer stabilization of the optimized amount of Ita3C_{12} monomers with MAPOSS cross-linkers in a LC medium under the electric field by irradiating UV light. The electro-optic properties of PS auto-MDVA cells were significantly enhanced after polymer stabilization. It was realized that the good mechanical and chemical stabilities of PS auto-MDVA layers were mainly due to the polymerized Ita3C_{12}/MAPOSS protrusions on the solid substrates and the pretilted host NLC medium. Additionally, we investigated the automatic formation of protrusions by utilizing the combined techniques of X-ray photoelectron spectroscopy (XPS), atomic force microscopy (AFM), and scanning electron microscopy (SEM).

RESULTS AND DISCUSSION

Chemical and Morphological Studies of the PS Auto-MDVA Cell. Ita3C_{12} monomers were synthesized and polymerized with MAPOSS cross-linkers for the construction of the PS auto-VA layer in the NLC cell. The concentrations of Ita3C_{12} monomers and MAPOSS cross-linkers were optimized for the fabrication of the auto-VA layer on the entire area of the LC cell without generating any light scatterings (Figure S1). The PS auto-VA layers exhibited a strong surface anchoring energy (1.404×10^{-4} J/m^2) similar to the conventional VA layers and the mechanical properties that were thermally stable even if the temperature of the host NLC was increased to T_{NI}.[1]

To confirm the chemical stability of the PS auto-VA layer, the Ita3C_{12}/MAPOSS/LC mixture was filled in a couple of cells. Both of them showed uniform dark states (Figure S2a,d). One of the LC cells was exposed to UV light for polymer stabilization, whereas another LC cell was retained without UV treatment for comparison. After the polymer-stabilization process in the former LC cell, the host NLC medium was removed by a solvent mixture (methylene chloride (MC)/*n*-hexane = 1/4). The disassembled LC cells were washed with organic solvents, such as chloroform, MC, *n*-hexane, and acetone and reassembled. Thereafter, pure LC was injected into the reassembled LC cells. The PS auto-VA cell showed uniform dark states even after the reassembly process (Figure S2e). According to the conoscopic polarized optical microscopy (POM) image represented in the inset of orthoscopic POM image, the pure LC in the reassembled LC cell was vertically aligned (Figure S2f). On the other hand, the auto-VA cell without polymer stabilization showed a typical schlieren texture (Figure S2b,c). That means, the auto-VA layer was stable against organic solvent attacks and was fixed on substrates after polymer stabilization. Furthermore, to investigate the elemental composition of the PS auto-VA layer located on the substrates of the LC cell, the fabricated PS auto-VA cells were disassembled and those substrates were examined with XPS.[27−29] The XPS data for the PS auto-VA layers on the substrates is represented in Figure 1. As shown Figure 1a, C−C bond, C−O bond, and C═O bond peaks were located on 284.8, 286, and 289 eV, respectively. The C−C bonds were alkyl chains of Ita3C_{12} and MAPOSS, and the C−O and C═O bonds were in the ester and carboxylic groups of ItaC_{12} and MAPOSS.[27] In the case of oxide (O 1s scans), Si−O and metal oxide peaks were located at 532.9 and 530 eV, respectively (Figure 1b). The Si−O peak proved the presence of MAPOSS as well as the glass area of the substrates. Note that both

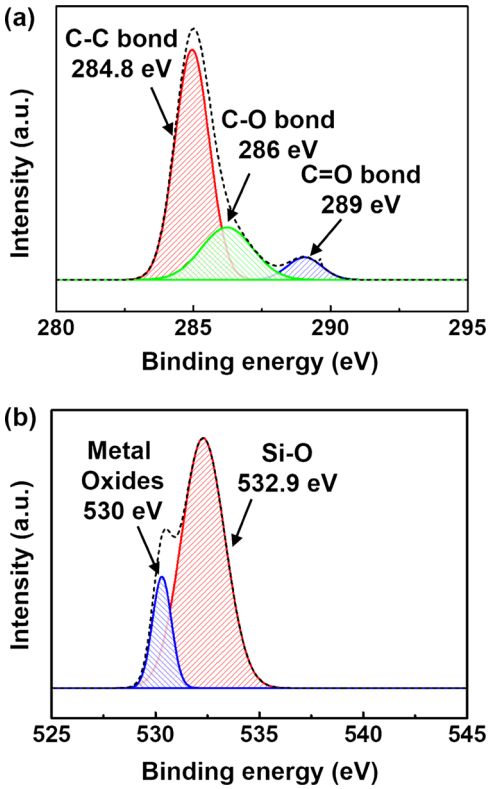

Figure 1. XPS spectra for the surface of the PS auto-VA cell: (a) carbon (C 1s) and (b) oxide (O 1s) spectra of chemical binding energy at the protrusions on the substrates obtained after washing the unpolymerized host LC medium.

MAPOSS and glass were composed of Si−O bonds.[28,29] The metal oxide peaks were detected on the electrodes of the substrates. The XPS result indicated the fact that the PS auto-VA layer located on the substrates of LC cells was composed of polymerized Ita3C_{12}/MAPOSS and fixed on the substrates. The PS auto-VA layer was quite stable against chemical attacks even after the disassembly.

In previous research, we investigated the surface morphology of the PS auto-VA layer on the substrates of the LC cell by AFM and recognized that the PS auto-VA layer was composed of nanosized protrusions (Figure 2).[1] In this study, to enhance electro-optic properties of the PS auto-VA layer, the multi-domain electrode cell designed for inducing the formation of a multidomain LC medium and wide viewing angle was used and Ita3C_{12} and MAPOSS in the LC medium were polymerized under an electric field for generating pretilted LC directors. Furthermore, to investigate the surface morphology of the PS auto-VA layer on the substrates of the multidomain electrode cell, the PS auto-MDVA layer was observed by AFM and field emission scanning electron microscopy (FE-SEM). When the auto-VA layer was constructed, Ita3C_{12} and MAPOSS were phase-separated and gradually migrated onto the substrates. However, Ita3C_{12} self-assembled as a dimer by intermolecular hydrogen bonding between carboxylic acids of Ita3C_{12} and the dimers were still dissolved in the host LC medium and aligned parallel to the host LC molecules, as shown in Figure 3a. After the construction of the auto-VA layer, electric field was applied to the fabricated auto-VA LC cell (Figure 3b). Under the square-waveform electric field at 5.6 V, Ita3C_{12} and MAPOSS located on the substrates and in the LC medium were polymerized by irradiating UV light (Figure 3c). Finally, when

DOI: 10.1021/acsomega.7b01015
ACS Omega 2017, 2, 5942−5948

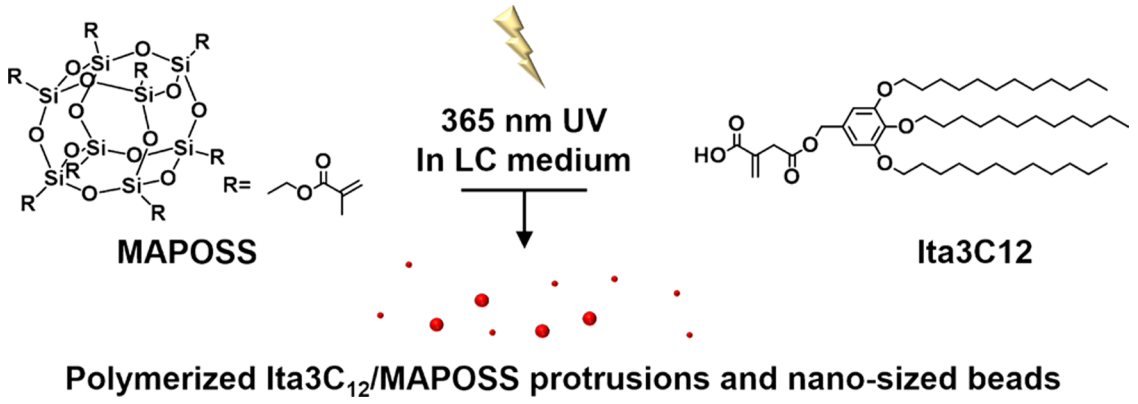

Figure 2. Formation of protrusions and nanosized beads during polymer stabilization.

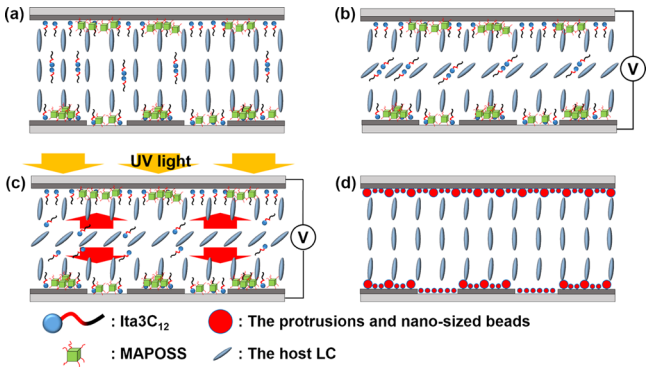

Figure 3. Schematic illustrations for the fabrication of the PS auto-MDVA cell. (a) Before polymer stabilization without an electric field, $Ita3C_{12}$ and MAPOSS are migrated on the electrode substrates and induce LC vertical alignment. The self-assembled $Ita3C_{12}$ dimers are still dissolved in the host LC medium. (b) Before polymer stabilization at the voltage of 5.6 V, directors of $Ita3C_{12}$ dimers and the host LC medium are reoriented along the applied electric field. (c) Polymer stabilization of $Ita3C_{12}$ and MAPOSS at the voltage of T_{90} by irradiating UV light: the self-assembled $Ita3C_{12}$ dimers and MAPOSS also reacted with each other, and the polymerized $Ita3C_{12}$/MAPOSS beads in the host LC medium are migrated into the electrode substrates. (d) After polymer stabilization and without electric field: the host LC molecules memorize the pretilt angles (about 2°) from vertical alignment even after removing the electric field.

the electric field was removed, the directors of host LC were aligned vertically with a slight pretilt angle (about 2°) (Figure 3d).[21−26] Note that the multidomain electrode substrates were consisted of prominent electrode areas based on indium tin oxide (ITO) and nonelectrode areas based on silicon oxide of the glass area of substrates.

For investigating the protrusions on the substrate in detail, FE-SEM was used. According to FE-SEM images (Figure 4), after the construction of the auto-MDVA layer, the VA layer on the electrode areas exhibited the protrusions with 37 nm width in averaged values (Figure 4a). On the other hand, the VA layer on the nonelectrode areas exhibited the protrusions with 17 nm width in averaged values (Figure 4b). From this result, several explanations were postulated that the sizes of the protrusions were influenced by several factors, such as elastic energy distribution of the host LC medium, caused under electric field, and chemical affinity between MAPOSS and the materials of the substrate. The elastic energy of the host LC medium is changed gradually when the host LC molecules are reoriented under an electric field.[30−35] To prove experimentally whether the electric field influenced the determination of the sizes of protrusions, $Ita3C_{12}$ and MAPOSS were polymerized in the multidomain electrode cell without applying electric field. The identical result was obtained, as shown in Figure S3. After polymerizing $Ita3C_{12}$ and MAPOSS without applying electric field, the protrusions on the electrode areas exhibited 37 nm width in averaged values (Figure S3b) and those on the nonelectrode areas exhibited 17 nm width in averaged values (Figure S3c). The widths of protrusions which are polymerized without and with the electric field were matched up. It means that the elastic energy change of the LC medium did not affect the determination of the sizes of the protrusions on the substrates. To test other speculations, the height of protrusions was measured by AFM.[36−38] As represented in Figure 5, the topographic AFM images and their corresponding height profiles of the protrusions on the substrates indicated that the heights of the protrusions on the electrode areas were higher than those on the nonelectrode areas. The heights of prominent electrodes were about 80 nm. After the construction

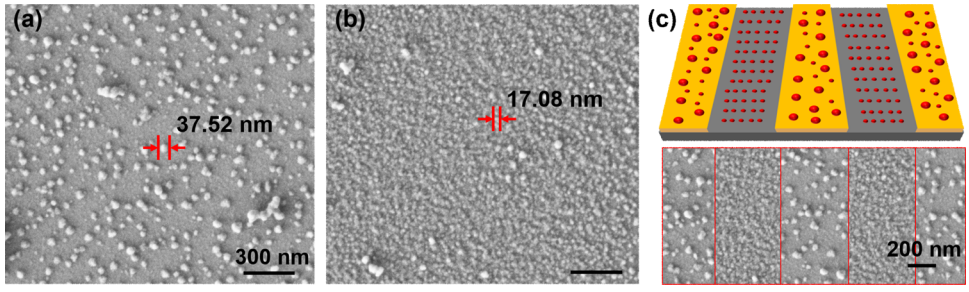

Figure 4. Topographic SEM images of the protrusions that were polymerized under electric field: on (a) and between (b) the electrodes. (c) Schematic diagram of the protrusions formed on the multidomain electrode substrate and its corresponding SEM image of the protrusions.

DOI: 10.1021/acsomega.7b01015
ACS Omega 2017, 2, 5942−5948

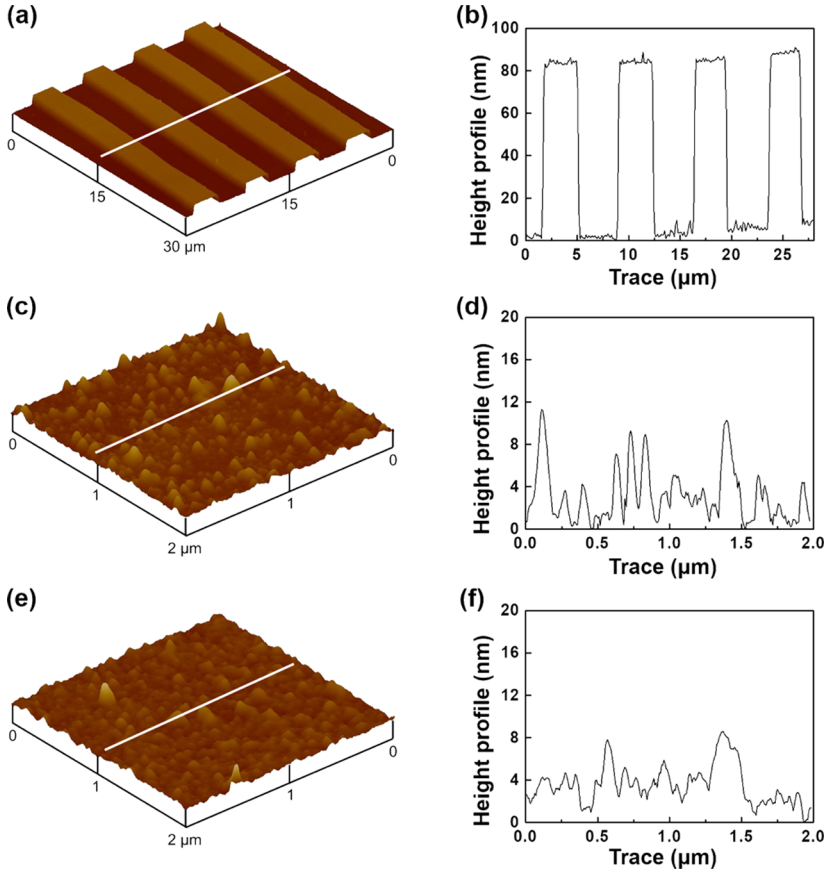

Figure 5. Topographic AFM images of the (a) multidomain electrode substrate, (c) surface of the electrode areas, and (e) surface of nonelectrode areas and (b, d, f) their corresponding height profiles, respectively.

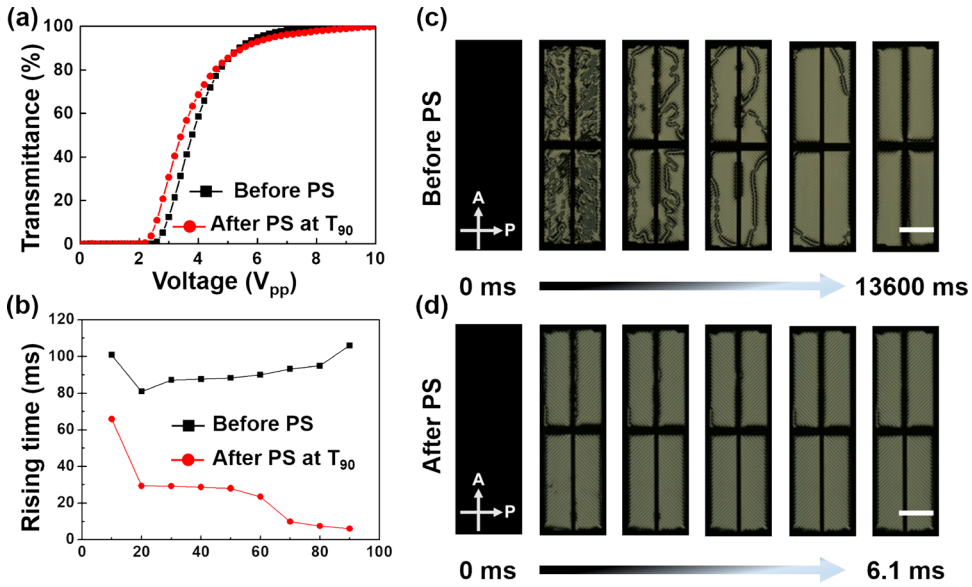

Figure 6. (a) Voltage-dependent transmittance curves before and after polymer stabilization at 5.6 V, and (b) rising time vs grayscale for the PS auto-MDVA LC cell before and after polymer stabilization. The time-resolved LC textures at 5.6 V (c) before and (d) after polymer stabilization, where the white scale bars correspond to 100 μm.

of the PS auto-VA layer, the VA layer on the electrode areas exhibited the protrusions with 8 nm height in averaged values (Figure 5c,d). On the other hand, the VA layer on the nonelectrode areas exhibited the protrusions with 4 nm height in averaged values (Figure 5e,f). From AFM and FE-SEM images, we discovered that some protrusions were existed on the electrode and nonelectrode areas as nanosized beads smaller than the protrusions on the nonelectrode areas (Figure 5d,f). These results can be supported by two mechanisms. The first is the chemical affinity of MAPOSS and the materials of

DOI: 10.1021/acsomega.7b01015
ACS Omega 2017, 2, 5942−5948

the substrate. When the LC mixture was injected into the fabricated multidomain electrode cell, automatic phase separation and subsequent migration onto substrates were induced because of the low solubility of MAPOSS in the host LC medium. The MAPOSS and nonelectrode areas were consisted of silicon atoms; however, the electrode areas were not. Therefore, MAPOSS and the nonelectrode areas have more chemical affinity than that of the electrode areas. As a result, MAPOSS molecules on the electrode areas were more aggregated themselves than those on nonelectrode areas (Figure 3a). When Ita3C$_{12}$ and MAPOSS in the fabricated multidomain electrode LC cell were polymerized by UV, the protrusions on the electrode areas were bigger than those on the nonelectrode areas (Figure 3d). The second is phase separation induced by the polymerization of Ita3C$_{12}$ and MAPOSS in the host LC medium. When Ita3C$_{12}$ and MAPOSS in the LC medium were polymerized by irradiating UV light, nanosized beads were formed in the LC medium. The nanosized beads were no longer dissolved in the LC medium, and phase separation against the LC medium was induced by low solubility. Then, the nanosized beads of 2−4 nm were gradually migrated onto the entire surfaces regardless of the substrate materials. As a result, we confirmed that polymerizations were occurred in the host LC medium and on the substrates of the LC cell simultaneously.

Improved Electro-Optic Properties of the PS Auto-MDVA Cell. POM images and voltage-dependent transmittance (VT) curves of the fabricated PS auto-MDVA cell with the pretilt angle were investigated to confirm the enhancement of electro-optic properties, such as threshold voltage and response times. The threshold voltage can be defined as the applied voltage when the LC cell has 10% of the maximum transmittance.[39−42] The threshold voltage is an important factor in determining how much energy is required to reorient the directors of the LC medium. A decrease in the threshold voltage can be evidence for the fact that the director of the LC medium is slightly tilted. Acorrding to voltage-transmittance curves in Figure 6a, the threshold voltage after polymer stabilization was decreased about 0.36 V at the voltage of 10% maximum of transmittance. The applied electric field range was from 0 to 10 V.

For the observation of time-resolved LC textures, POM images were obtained before and after polymer stabilization with the voltage applied. Both the LC cells before and after polymer stabilization maintained the dark states without applying any electric fields. This indicated that the host LC was vertically aligned in initial states and the LC directors were even slightly tilted after polymer stabilization. Before polymer stabilization, LC directors were not tilted. Consequently, the LC molecules without polymer stabilization were bumped with themselves while applying the higher electric field than the threshold voltage.[21−26] Therefore, the LC cell before polymer stabilization has a long time to reorient the LC texture perfectly. When the electric field (5.6 V) was applied across the auto-MDVA cell before polymer stabilization, schlieren textures were perfectly disappeared after 13 600 ms (Figure 6c). In contrast, the PS auto-MDVA cell did not exhibit Schlieren textures anymore and the response time of the reorientation of LC directors at 5.6 V applied state was about 2000 times faster than before polymer stabilization (6.1 ms). The results clearly indicate that the electro-optic properties of the PS auto-MDVA cell are significantly enhanced by the pretilt angle of the host LC medium.

CONCLUSIONS

For automatically fabricating the polymer-stabilized (PS) multidomain vertical alignment (MDVA) layer with a pretilt angle (PS auto-MDVA), Ita3C$_{12}$ monomers with MAPOSS cross-linkers were photopolymerized in the LC medium under the electric field by irradiating UV light. The fabricated PS auto-MDVA cell exhibited improved electro-optic properties, such as lower threshold voltage, faster response time, and wider viewing angle, which were mainly resulted from the induced pretilt angle and the multidomain states of host LC molecules. On the basis of the morphological observations combined with surface chemical analyses, it was found that the protrusions formed on the electrode areas (37 nm width and 8 nm height) were bigger than those on the nonelectrode areas (17 nm width and 4 nm height) and the final surface morphology was determined by the two-step mechanisms. Because of the different chemical affinities between MAPOSS and the substrate materials, the diffused MAPOSS on the electrode areas was first aggregated to form bigger nanosized droplets rather than those on the nonelectrode areas. Second, smaller nanosized beads were formed during the photopolymerization of dissolved Ita3C$_{12}$ and MAPOSS. The smaller nanosized beads were further phase-separated against the host LC medium and gradually diffused onto the entire substrates regardless of the chemical affinities between MAPOSS and the substrate materials. We successfully demonstrated a PS auto-MDVA cell with enhanced electro-optic properties and additionally investigated the two-step mechanisms for the automatic formation of protrusions on the multidomain electrode substrates during polymer stabilization.

EXPERIMENTAL SECTION

Materials. 1-Bromododecane (97%, Aldrich), methyl 3,4,5-trihydroxybenzoate (98%, Aldrich), itaconic anhydride (95%), methacryl polyhedral oligomeric silsesquioxane (Hybrid Plastics), lithium aluminum hydride (95%, Aldrich), anhydrous chloroform (99%, Sigma-Aldrich), acetone (99.5%, Showa), methylene chloride (99%, Showa), *n*-hexane (99.5%, Showa), and nematic liquid crystal (NLC, ZSM-7232XX, $\Delta\varepsilon = -3.4$, $\Delta n = 0.101$, LIXON) were used as received.

Synthesis. The itaconic acid-based dendritic amphiphile monomer (Ita3C$_{12}$) was synthesized according to a previously described method.[1]

Preparation of the Auto-VA Cell and Auto-MDVA Cell. The PS auto-VA test cells were fabricated by sandwiching two bare electrode substrates. The bare electrode substrates were washed several times with distilled water, isopropyl alcohol, and acetone. The washed electrode substrates were further dried in a high-vacuum oven at 80 °C for 3 h. Two cleaned electrode substrates were attached to each other and sealed with 5 μm cell gap tapes. The dimensions of the auto-VA cell were 1.5 cm × 1.5 cm. The empty cells were filled with the NLC mixture (NLC/Ita3C$_{12}$/MAPOSS = 99.5/0.4/0.1 wt %). The LC mixture was prepared by stirring at 60 °C for 1 day.

The PS auto-MDVA cells were also fabricated by sandwiching the nonpatterned ITO glass (upper one) and the multidomain electrode substrate (downward one) provided by a display company. The multidomain electrode substrates were carefully washed several times with distilled water, isopropyl alcohol, and acetone and then dried in a vacuum oven at 80 °C for 3 h. The cell gap of the fabricated cell was maintained to be 5 μm by cell gap tapes. The typical

DOI: 10.1021/acsomega.7b01015
ACS Omega 2017, 2, 5942−5948

dimensions of the auto-MDVA cell were 2 cm × 2 cm. The homogenous LC mixture was injected into the cells by capillary forces.

Characterization. Proton nuclear magnetic resonance (^{1}H NMR) spectra were recorded on a JNM-EX400 spectrometer in deuterated chloroform ($CDCl_3$) at room temperature. Chemical shifts were quoted in parts per million (ppm) and referenced to tetramethylsilane. Orthoscopic microphotographs and conoscopic textures were taken by using cross-polarized optical microscopy (POM, Nikon ECLIIPSE E600POL) with a LINKAM LTS 350 heating stage. Atomic force microscopy (AFM) images were taken on an Agilent 550 AFM (Agilent technologies) using silicon cantilevers with spring constants of 20−30 N/m. The scan speed varied from 0.0 to 1.0 line/s, and the resonance frequencies were set as 140−160 kHz. The contact angle was measured by a contact angle analyzer (Phoenix-300, SEO). Electro-optical switching behaviors were measured by LCMS-200 (Sesim Photonics Technology, Korea). A scanning electron microscope (SUPRA 40VP, Carl Zeiss) and an X-ray photoelectron spectroscope (K-Alpha, Thermo Scientific) were utilized for morphological and chemical investigations, respectively.

■ ASSOCIATED CONTENT

Supporting Information

The Supporting Information is available free of charge on the ACS Publications website at DOI: 10.1021/acsomega.7b01015.

POM and FE-SEM results and detailed experimental processes (PDF)

■ AUTHOR INFORMATION

Corresponding Author

*E-mail: kujeong@jbnu.ac.kr.

ORCID

Kwang-Un Jeong: 0000-0001-5455-7224

Author Contributions

The article was written through contributions of all authors. All authors have given approval to the final version of the manuscript.

Notes

The authors declare no competing financial interest.

■ ACKNOWLEDGMENTS

This work has been supported by BRL (2015042417), MOTIE-KDRC (10051334), and Mid-Career Researcher Program (2016R1A2B2011041) of Korea. W.-J.Y. appreciates support from the NRF-2017 Global Ph.D. Fellowship Program.

■ REFERENCES

(1) Yoon, W. J.; Choi, Y. J.; Kim, D. Y.; Kim, J. S.; Yu, Y. T.; Lee, H. J.; Lee, J. H.; Jeong, K. U. Photopolymerization of Reactive Amphiphiles: Automatic and Robust Vertical Alignment Layers of Liquid Crystals with a Strong Surface Anchoring Energy. *Macromolecules* **2016**, *49*, 23−29.

(2) Wang, S.; He, J.; Zeng, Y.; Yan, B.; Wang, Y. Effect of polymer structures on electro-optical properties of polymer stabilized liquid crystal films. *Front. Chem. Eng. China* **2008**, *2*, 265−268.

(3) Dierking, I. Polymer Network-Stabilized Liquid Crystals. *Adv. Mater.* **2000**, *12*, 3.

(4) Rajaram, C. V.; Hudson, S. D.; Chien, L. C. Morphology of Polymer-Stabilized Liquid Crystals. *Chem. Mater.* **1995**, *7*, 2300−2308.

(5) Dierking, I.; Kosbar, L. L.; Afzali-Ardakani, A.; Lowe, A. C.; Held, G. Network morphology of polymer stabilized liquid crystals. *Appl. Phys. Lett.* **1997**, *71*, 2454−2456.

(6) Hwang, B. H.; Ahn, H. J.; Rho, S. J.; Chae, S. S.; Baik, H. K. Vertical Alignment of Liquid Crystals with Negative Dielectric Anisotropy on an Inorganic Thin Film with a Hydrophilic Surface. *Langmuir* **2009**, *25*, 8306−8312.

(7) Seo, D.-S.; Lee, J.-H. Wide Viewing Angle and Fast Response Time Characteristics of Nematic Liquid Crystal Using Novel Vertical-Alignment-1/4π Cell Mode on Homeotropic Alignment Layer. *Jpn. J. Appl. Phys.* **1999**, *38*, L1432−L1434.

(8) Lee, S. H.; Lee, M. H. Liquid Crystals Displays with High Image Quality and Fast Response Time. *J. Korean Phys. Soc.* **2001**, *39*, 42−48.

(9) Lee, S. H.; Bhattacharyya, S. S.; Jin, H. S.; Jeong, K. U. Devices and materials for high-performance mobile liquid crystal displays. *J. Mater. Chem.* **2012**, *22*, 11893.

(10) Lee, W. K.; Choi, Y. S.; Kang, Y. G.; Sung, J.; Seo, D. S.; Park, C. Super-Fast Switching of Twisted Nematic Liquid Crystals on 2D Single Wall Carbon Nanotube Networks. *Adv. Funct. Mater.* **2011**, *21*, 3843−3850.

(11) Zhou, J.; Collard, D. M.; Park, J. O.; Srinivasarao, M. Control of the Anchoring Behavior of Polymer-Dispersed Liquid Crystals: Effect of Branching in the Side Chains of Polyacrylates. *J. Am. Chem. Soc.* **2002**, *124*, 9980−9981.

(12) Kang, Y. G.; Kim, H. J.; Park, H. G.; Kim, B. Y.; Seo, D. S. Tin dioxide inorganic nanolevel films with different liquid crystal molecular orientations for application in liquid crystal displays. *J. Mater. Chem.* **2012**, *22*, 15969−15975.

(13) Oh-e, M.; Kondo, K. Response mechanism of nematic liquid crystals using the in-plane switching mode. *Appl. Phys. Lett.* **1996**, *69*, 623−625.

(14) Lee, S. H.; Lee, S. L.; Kim, H. Y. Electro-optic characteristics and switching principle of a nematic liquid crystal cell controlled by fringe-field switching. *Appl. Phys. Lett.* **1998**, *73*, 2881.

(15) Yu, I. H.; Song, I. S.; Lee, J. Y.; Lee, S. H. Intensifying the density of a horizontal electric field to improve light efficiency in a fringe-field switching liquid crystal display. *J. Phys. D: Appl. Phys.* **2006**, *39*, 2367.

(16) Liu, B. Y.; Chen, L. J. Role of Surface Hydrophobicity in Pretilt Angle Control of Polymer-Stabilized Liquid Crystal Alignment Systems. *J. Phys. Chem. C* **2013**, *117*, 13474−13478.

(17) Schiekel, M. F.; Fahrenschon, K. Deformation of Nematic Liquid Crystals with Vertical Orientation in Electrical Fields. *Appl. Phys. Lett.* **1971**, *19*, 391.

(18) Geary, J. M.; Goodby, J. W.; Kmetz, A. R.; Patel, J. S. The Mechanism of polymer alignment of liquid-crystal materials. *J. Appl. Phys.* **1987**, *62*, 4100.

(19) Kim, S. G.; Kim, S. M.; Kim, Y. S.; Lee, H. K.; Lee, S. H.; Lee, G.-D.; Lyu, J.-J.; Kim, K. H. Stabilization of the liquid crystal director in the patterned vertical alignment mode through formation of pretilt angle by reactive mesogen. *Appl. Phys. Lett.* **2007**, *90*, No. 261910.

(20) Zhao, D.; Huang, W.; Cao, H.; Zheng, Y.; Wang, G.; Yang, Z.; Yang, H. Homeotropic Alignment of Nematic Liquid Crystals by a Photocross-Linkable Organic Monomer Containing Dual Photofunctional Groups. *J. Phys. Chem. B* **2009**, *113*, 2961−2965.

(21) Huang, C. Y.; Jhuang, W. Y.; Hsieh, C. T. Switching of polymer-stabilized vertical alignment liquid crystal cell. *Opt. Express* **2008**, *16*, 3859−3864.

(22) Lim, S. H.; Kim, D. H.; Shin, S. J.; Woo, W. C.; Jin, H. S.; Lee, S. H.; Kim, E. Y.; Lee, S. E. P-143: Polymer Stabilized In-Plane Field Driven Vertical Alignment Liquid Crystal Device. *SID Symp. Dig. Tech. Pap.* **2011**, *42*, 1645−1647.

(23) Hwang, S. J.; Kim, S. M.; Srivastava, A. K.; Lee, M. H.; Lee, S. H.; Lyu, J. J.; Kim, K. H.; Lu, R.; Wu, S. T. Surface Polymer-Stabilized Vertically Aligned Liquid Crystal Cells with Various Polymer Wall Structures. *Mol. Cryst. Liq. Cryst.* **2008**, *489*, 563−571.

(24) Hicks, S. E.; Hurley, S. P.; Zola, R. S.; Yang, D. K. Polymer Stabilized VA mode Liquid Crystal Display. *J. Disp. Technol.* **2011**, *7*, 619−623.

DOI: 10.1021/acsomega.7b01015
ACS Omega 2017, 2, 5942−5948

(25) Chen, T. J.; Lin, G. J.; Chen, B. Y.; Lin, B. R.; Wu, J. J.; Ying, Y. J. Optimized electro-optical properties of polymer-stabilized vertical-aligned liquid crystal displays driven by an in-plane field. *Displays* **2015**, *37*, 94−99.
(26) Weng, L.; Liao, P. C.; Lin, C. C.; Ting, T. L.; Hsu, W. H.; Su, J. J.; Chien, L. C. Anchoring energy enhancement and pretilt angle control of liquid crystal alignment on polymerized surfaces. *AIP Adv.* **2015**, *5*, No. 097218.
(27) Hsu, H.-L.; Leong, K. R.; Teng, I. J.; Halamicek, M.; Juang, J. Y.; Jian, S. R.; Qian, L.; Kherani, N. P. Reduction of Photoluminescence Quenching by Deuteration of Ytterbium-Doped Amorphous Carbon-Based Photonic Materials. *Materials* **2014**, *7*, 5643−5663.
(28) Wang, W.; Chen, C.; Zhang, G.; Wang, T.; Wu, H.; Liu, Y.; Liu, C. The function of a 60-nm-thick AlN buffer layer in n-ZnO/AlN/p-Si(111). *Nanoscale Res. Lett.* **2015**, *10*, 91.
(29) Singh, S. D.; Ajimsha, R. S.; Sahu, V.; Kumar, R.; Misra, P.; Phase, D. M.; Oak, S. M.; Kukreja, L. M.; Ganguli, T.; Deb, S. K. Band alignment and interfacial structure of ZnO/Ge heterojunction investigated by photoelectron spectroscopy. *Appl. Phys. Lett.* **2012**, *101*, No. 212109.
(30) Kim, S. D.; Lee, B.; Kang, S. W.; Song, J. K. Dielectrophoretic manipulation of the mixture of isotropic and nematic liquid. *Nat. Commun.* **2015**, *6*, No. 7936.
(31) Ohkawa, S.; Ohta, R.; Kawabata, K.; Goto, H. Polymerization in Liquid Crystal Medium: Preparation of Polythiophene Derivation Bearing a Bulky Pyrimidine Substituent. *Polymers* **2010**, *2*, 393−406.
(32) Iseki, T.; Kawabata, K.; Kawashima, H.; Goto, H. Catalysis direction selective asymmetric polymerization in chiral liquid crystal medium. *Polymer* **2014**, *55*, 66−72.
(33) Belamie, E.; Mosser, G.; Gobeaux, F.; Giraud-Guille, M. M. Possible Transient liquid crystal phase during the laying out of connective tissues: α-chitin and collagen as models. *J. Phys.: Condens. Matter* **2006**, *18*, S115−S129.
(34) Sova, O.; Reshetnyak, V.; Galstian, T.; Asatryan, K. Electrically variable liquid crystal lens based on the dielectric dividing principle. *J. Opt. Soc. Am. A* **2015**, *32*, 803−808.
(35) Ackerman, P. J.; Qi, Z.; Lin, Y.; Twombly, C. W.; Laviada, M. J.; Lansac, Y.; Smalyukh, I. I. Laser-directed hierarchical assembly of liquid crystal defects and control of optical phase singularities. *Sci. Rep.* **2011**, *2*, No. 414.
(36) Kundu, S.; Lee, M. H.; Lee, S. H.; Kang, S. W. In Situ Homeotropic Alignment of Nematic Liquid Crystals Based on Photoisomerization of Azo-Dye, Physical Adsorption of Aggregates, and Consequent Topographical Modification. *Adv. Mater.* **2013**, *25*, 3365−3370.
(37) Hahm, S. G.; Ko, Y. G.; Rho, Y.; Ahn, B.; Ree, M. Liquid crystal alignment in advanced flat-panel liquid crystal displays. *Curr. Opin. Chem. Eng.* **2013**, *2*, 71−78.
(38) Berreman, D. W. Solid Surface Shape and the Alignment of Adjacent Nematic Liquid Crystal. *Phys. Rev. Lett.* **1972**, *28*, 1683−1686.
(39) Choi, S. W.; Jin, H.; Kim, K. H.; Lee, J. H.; Kim, H.; Shin, K. C.; Kim, H. S.; Yoon, T. H. Formation of Dual Threshold in a Vertical Alignment Liquid Crystal Device. *J. Opt. Soc. Korea* **2012**, *16*, 170−173.
(40) Ma, H.; Yang, R.; Sun, Y. The optical threshold and saturation voltage of blue-phase liquid crystal display with uniform operating electric field. *Liq. Cryst.* **2015**, *42*, 1743−1747.
(41) Bryan-Brown, G. P.; Brown, C. V.; Sage, I. C.; Hui, V. C. Voltage-dependent anchoring of a nematic liquid crystal on a grating surface. *Nature* **1998**, *392*, 365−367.
(42) Malik, M. K.; Bhatia, P. G.; Deshmukh, R. R. Effect of nematic liquid crystals on optical properties of solvent induced phase separated PDLC composite films. *Indian J. Sci. Technol.* **2012**, *5*, 3440−3452.

DOI: 10.1021/acsomega.7b01015
ACS Omega 2017, 2, 5942−5948